Photodissociation dynamics of acetylene via the $\tilde{C}\ ^1\Pi_u$ electronic state

Yongwei Zhang,[1,2] Kaijun Yuan,[1,a)] Shengrui Yu,[1] David H. Parker,[2] and Xueming Yang[1,a)]
[1]*State key Laboratory of Molecular Reaction Dynamics, Dalian Institute of Chemical Physics, Chinese Academy of Sciences, 457 Zhongshan Road, Dalian 116023, China*
[2]*Institute for Molecules and Materials, Radboud University Nijmegen, Heijendaalseweg 135, 6525 ED Nijmegen, The Netherlands*

(Received 16 March 2010; accepted 3 June 2010; published online 7 July 2010)

Photodissociation of acetylene has been studied using the H-atom Rydberg tagging time-of-flight technique at two excitation wavelengths (148.35 and 151.82 nm) in the vacuum ultraviolet region. Product translational energy distributions have been obtained from the H-atom time-of-flight spectra. Experimental results indicate that the C_2H product is mainly populated in the $\tilde{A}$ state. Clear *trans*-bend ν_2 and C–C stretch ν_3 vibrational progressions of the $C_2H(\tilde{A})$ product in the product internal energy distribution were observed. The anisotropy parameter obtained from experiment is clearly translational energy dependent for both photolysis wavelengths. The anisotropy parameters at the two photolysis wavelengths were also found to be significantly different from each other, suggesting different dissociation dynamics for the two photolysis wavelengths. © *2010 American Institute of Physics*. [doi:10.1063/1.3456738]

I. INTRODUCTION

Acetylene (C_2H_2) has received considerable attention because of its importance in the field of planetary atmosphere[1,2] and hydrocarbon combustion chemistry[3] in past several decades. The photochemistry and dissociation dynamics of acetylene in the ultraviolet (UV) region has been extensively studied. However, photochemistry of acetylene in the vacuum ultraviolet (VUV) region has not been well studied because of the lack of intense tunable VUV sources. In the region below the first ionization limit, different photodissociation processes can lead to the following dissociation channels:

$$C_2H_2 \rightarrow C_2H + H \quad D_0 = 46\,074\ \text{cm}^{-1}, \tag{1}$$

$$C_2H_2 \rightarrow C_2 + H_2 \quad D_0 = 50\,000\ \text{cm}^{-1}, \tag{2}$$

$$C_2H_2 \rightarrow CH + CH \quad D_0 = 79\,800\ \text{cm}^{-1}. \tag{3}$$

Among the above channels, previous experimental studies performed at different excitation wavelengths have shown that the dissociation of acetylene is dominated by process (1).[4]

Spectroscopic studies of acetylene are abundant in the UV and VUV region. The 190–240 nm spectrum is assigned to the $\tilde{A}\ ^1A_u \leftarrow \tilde{X}\ ^1\Sigma_g$ electronic transition.[5,6] The C–C stretch mode ν_2' and the *trans*-bend mode ν_3' of C_2H_2 are both excited as the transition from linear ground state to *trans*-bent first excited state.[7] Photodissociation of C_2H_2 via excited $\tilde{A}\ ^1A_u$ state at 193.3 nm has been carried out separately by means of mass spectrometric detected time-of-flight (TOF) method[8,9] and H-atom Rydberg tagging time-of-flight (HRTOF) technique.[10] The ground state $C_2H(\tilde{X}\ ^2\Sigma^+)$ product was found to be dominant,[8–11] while a few vibrational states of $C_2H(\tilde{A}\ ^2\Pi)$ were also observed. Experimental results also indicate that vibrationally excited $C_2H(\tilde{A}\ ^2\Pi)$ products are more prominent at shorter wavelengths.[12,13] In the 165–190 nm VUV region, absorption spectrum is due to the $\tilde{B}\ ^1B_u \leftarrow \tilde{X}\ ^1\Sigma_g$ electronic transition.[14]

The hydrogen Lyman-α photodissociation of C_2H_2 at 121.6 nm has been studied using Doppler-selected TOF technique[15] and the H Rydberg atom TOF technique[16] separately, both experiments have confirmed that the transition near this wavelength can be assigned to the $(3\tilde{R}''(^1\Pi_u) \leftarrow \tilde{X}\ ^1\Sigma_g)$ (Ref. 17) transition in which $3\tilde{R}''(^1\Pi_u)$ is interpreted as a case of Rydbergization.[18] At this excitation wavelength, more vibrational modes (C–H stretch mode ν_1, C–C stretch mode ν_3, and *trans*-bend mode ν_2) of the C_2H radical are excited and some of those vibrational excited states could be assigned undoubtedly. For instance, two vibrational progressions (C–H stretching and C–C stretching) of $C_2H(\tilde{A})$ are observed, similar to $C_2H(\tilde{A})$ in a neon matrix study.[19] Additionally, according to both observations the stretching vibrational modes (ν_1 and ν_3) of the C_2H radical seem to be excited preferentially, in comparison with the bending levels ν_2. This is quite different from the previous results at long wavelength excitation.[10]

Experimental[17,20–22] and theoretical[23–25] spectroscopic studies concluded that the C_2H_2 spectra of near ~150 nm is due to the $\tilde{C}\ ^1\Pi_u \leftarrow \tilde{X}\ ^1\Sigma_g$ electronic transition.[16,26–28] Recently, Ashfold *et al.*[29] pointed out that the predissociating of $\tilde{C}\ ^1\Pi_u$ state of C_2H_2 at 157 nm was undergoing the $3s\sigma^* \leftarrow 1\pi$ Rydberg transitions which correlates diabatically with H plus $C_2H(A)$ products. The acetylene absorption spectrum around 150 nm is shown in Fig. 1.[22,30] The strongest peak around 152 nm in the spectrum is assigned to the

a)Authors to whom correspondence should be addressed. Electronic addresses: kjyuan@dicp.ac.cn and xmyang@dicp.ac.cn.

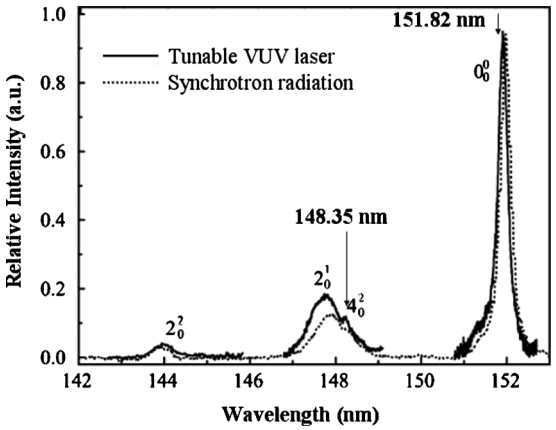

FIG. 1. Absorption spectrum of C_2H_2 molecule at the range of 142–153 nm. The solid line is for measurements of acetylene under jet-cooled condition with tunable VUV laser radiation (Ref. 19) and the dotted line is for the data recorded at room temperature by using synchrotron radiation (Ref. 26).

0_0^0 band. The peak around 148 nm in Fig. 1 is assigned to the 2_0^1 and 4_0^2 vibronic bands, which correspond to C–C stretch mode and *trans*-bending mode excitation. The peak at 144 nm is assigned to the 2_0^2 band. These spectroscopic studies show that the $\tilde{C}\ ^1\Pi_u$ state is strongly predissociative. No photodissociation study, however, has been carried out on this electronic excitation.

In this work, we present the experimental results of our recent photodissociation study at two VUV wavelengths using HRTOF technique,[31,32] in combination with a tunable VUV photolysis source.[33] The H-atom TOF spectra were measured at the two excitation wavelengths with different photolysis polarizations, the product translational energy distributions, or the internal energy distributions of C_2H, as well as the product angular distributions are derived. From these distributions, the dynamics of C_2H_2 photodissociation at the two wavelength excitations are distinctively different. The origins of the dynamical differences between the two wavelengths are then discussed.

II. EXPERIMENTAL

The photodissociation of C_2H_2 is studied using the high-*n* Rydberg H-atom time-of-flight (HRTOF) spectroscopy. The experimental setup has been described in details in a previous article,[34] and only a brief overview is given here. A sample of 2% acetylene in Ar is supersonically expanded into vacuum chamber via a pulsed general valve at a backing pressure of about 1100 Torr. The beam expansion goes through a 2 mm diameter skimmer. The acetylene beam was interrogated by the tunable VUV light beam (148.35 and 151.82 nm), as well as the Rydberg tagging laser beams (121.6 and 365 nm). The nascent H atom products at the ground n=1 level are excited to the n=2 state using the 121.6 nm VUV laser and subsequently to a high Rydberg state with n=30–80 using the 365 nm light. The charged species formed in the interaction region are extracted off by applying a small electric field (~20 V/cm) across the interaction region. The neutral Rydberg H atoms then fly about 740 mm to reach a fixed microchannel plate (MCP) detector. The Rydberg tagged atoms are immediately field-ionized by the electric field applied between the front plate of the Z-stack MCP detector and the fine metal grid. The TOF signal detected by the MCP is then amplified by a fast preamplifier, and counted by a multichannel scaler.

The laser system for generating the tunable VUV radiation as photolysis source and for the two-step Rydberg excitation is described previously.[33] The VUV photolysis light at 148.35 nm and 151.82 nm is generated by difference four-wave mixing of two 212.55 nm photons and one 352.94 nm photon or one 374.33 nm photon in a pure Krypton gas cell. The 212.55 nm used here is the same beam used for producing 121.6 nm light, which is generated by mixing two 212.55 nm photons and one 845 nm photon in the same Krypton cell. The 212.55 nm laser is generated by doubling the 355 nm output of a Nd:YAG (yttrium aluminum garnet) laser (Spectra Physics Pro-290, 30 Hz, 8–10 ns) pumped dye laser (Sirah, PESC-G-24) operating at ~425 nm. A portion of the 532 nm output of the same Nd:YAG laser is used to pump another dye laser (Continuum ND6000) which operates at ~845 nm. The 352.94 or 374.33 nm light for the tunable VUV photolysis light was generated by another Nd:YAG pumped dye laser system.

III. RESULTS AND DISCUSSIONS

A. Product translational energy distributions

TOF spectra of the H-atom product from photodissociation of C_2H_2 at 148.35 and 151.82 nm with laser polarization parallel and perpendicular to the detection axis have been measured using the experimental method described above (Fig. 2). TOF spectra of the H-atom product at the magic angle (54.7°) polarization are also measured to ensure that the intensity ratio of the TOF spectra obtained at both parallel and perpendicular polarization is correct. The TOF spectra are then converted into the total product translational energy distributions ($E_T(H)+E_T(C_2H)$) in the center-of-mass (COM) frame (Fig. 3).

Since the H-atom product has no internal excitation, the energies of the whole system can be described by the equation below

$$E_{hv} = D_0(H - C_2H) + E_T(H) + E_T(C_2H) + E_{int}(C_2H), \quad (4)$$

where E_{hv} is the energy of photolysis laser, $D_0(H-C_2H)$ is the bond energy of C–H which was determined to be 46 073.6(±7) cm^{-1} by previous experimental study,[35] $E_T(H)$, $E_T(C_2H)$, and $E_{int}(C_2H)$ stand for the translational energy of H atom, the translational energy of C_2H radical and the internal energy of C_2H radical respectively. $E_T(H)$ is related to $E_T(C_2H)$ by the momentum conservation law in the COM frame,

$$m_H E_T(H) = m_{C_2H} E_T(C_2H)). \quad (5)$$

Using above equation, internal state distribution of the C_2H radical can be determined from the total product translational energy distributions. Possible vibrational assignments of the C_2H radical have been made in the translation energy distributions shown in Fig. 3. From the translational energy distributions, it seems that there are three main vibrational progressions. The two main peaks at about 17 200 and

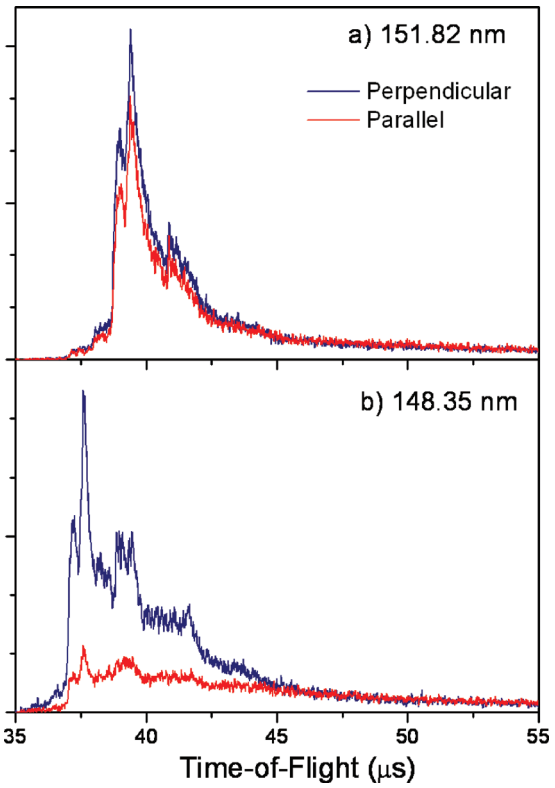

FIG. 2. TOF spectra of the H atom product from the photodissociation of C_2H_2 at 151.82 and 148.35 nm with photolysis laser polarization parallel and perpendicular to the detection axis.

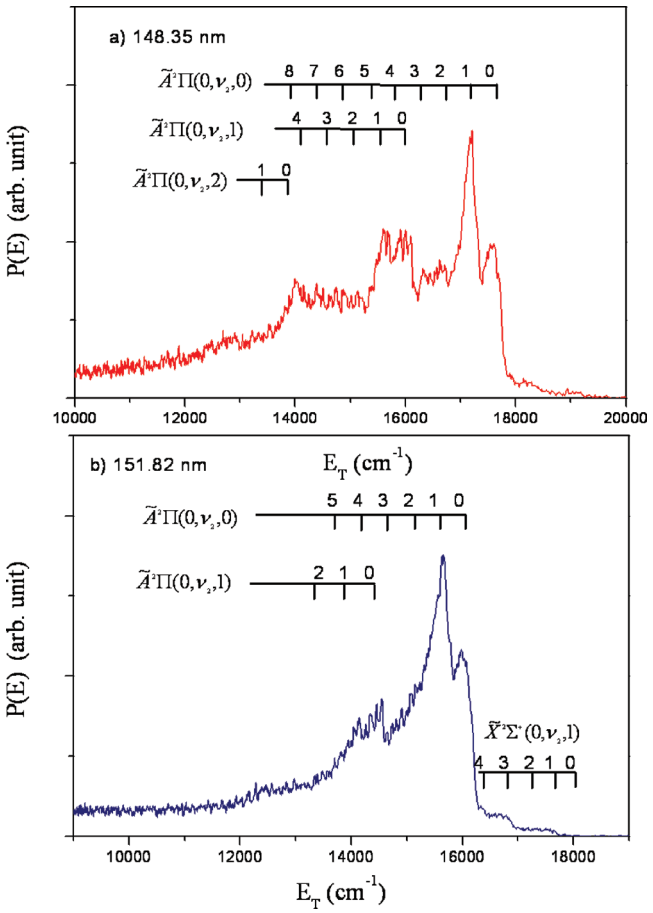

FIG. 3. Total translational energy spectra for 148.35 nm (a) and 151.82 nm (b) photodissociation with laser polarization perpendicular to detection axis and the assignment on the vibrational level of C_2H product.

17 550 cm^{-1} can be clearly assigned to the C_2H $\tilde{A}\,^2\Pi(0,\ v_2=0,\ v_3=0)$ and $\tilde{A}\,^2\Pi(0,\ 1,\ 0)$ levels, where v_2 is C–C–H bending vibration ($\sim$400 cm^{-1}) and v_3 is the C–C stretching vibration ($\sim$1800 cm^{-1}),[36] which is similar to the photodissociation results observed by Zhang and co-workers[10] at 193 nm photolysis; while structures at 16 000 and 14 000 cm^{-1} can be assigned to the $\tilde{A}\,^2\Pi(0,\ v_2,\ 1)$ and $\tilde{A}\,^2\Pi(0,\ v_2,\ 2)$ vibrational progressions. These assignments show that the dominant channel of the C_2H_2 photodissociation at both excitation wavelengths via the $\tilde{C}\,^1\Pi_u \leftarrow \tilde{X}\,^1\Sigma_g$ transition is the $C_2H(\tilde{A}\,^2\Pi)$ product plus an H-atom. Weak signals are also seen for $E_T \geq 17\,900$ cm^{-1}. These structures are possibly due to the $C_2H(\tilde{X}\,^2\Sigma^+(0,\ v_2 \leq 4,\ 1))$ structures, suggesting that the $C_2H(\tilde{X}\,^2\Sigma^+)$+H channel is very minor. It is also possible that these small structures are from the secondary photolysis of $C_2H(\tilde{A}\,^2\Pi)$ fragments.[9]

From the translational energy distribution, the $C_2H(\tilde{A}\,^2\Pi)$ product is obviously less vibrationally excited for photolysis at 151.82 nm via the 0_0^0 band excitation, than at 148.35 nm via the mixed 2_0^1 and 4_0^2 band excitation. An extra structure assigned to the progressions of $\tilde{A}\,^2\Pi(0,\ v_2,\ 2)$ is clearly observed at 148.35 nm photodissociation. Vibrational population in the $\tilde{A}\,^2\Pi(0,\ v_2,\ 1)$ states is also significantly enhanced. This means that the vibrationally excited C_2H_2 precursor in the $\tilde{C}\,^1\Pi_u$ state produces more vibrationally excited C_2H radical products in the C–C stretching and C–C–H bending vibrations. From the transitional energy distributions, the rotational excitation for the C_2H $\tilde{A}\,^2\Pi(0,\ 0,\ 0)$ and $\tilde{A}\,^2\Pi(0,\ 1,\ 0)$ product states seems to be not very hot, suggesting that the transition state to produce these products are not very far from the linear geometry.

B. Product angular anisotropy distributions

Since TOF spectra of the H atom products from the C_2H_2 photodissociation are measured for both parallel and perpendicular polarization, the anisotropy parameter β for the dissociation process is also determined from the equation

$$I(\theta) = (1/4\pi)(1 + \beta P_2(\cos\ \theta)), \tag{6}$$

where θ is the angle between the polarization direction and the detection axis, the $P_2(\cos\ \theta)$ is the second Legendre polynomial, β is the anisotropy parameter. Figure 4 shows the translational energy dependent product anisotropy parameter obtained at 148.35 and 151.82 nm photolysis. Clearly, the anisotropy parameters for the two photolysis wavelengths are translational energy dependent. The distributions for the two wavelengths are very different from each other. For 148.35 nm photolysis, the anisotropy parameter around $E_T = 17\,500$ cm^{-1} is about -0.74. This suggests that the photoexcitation is a perpendicular transition and the dissociation time is very fast in producing these low vibrationally excited

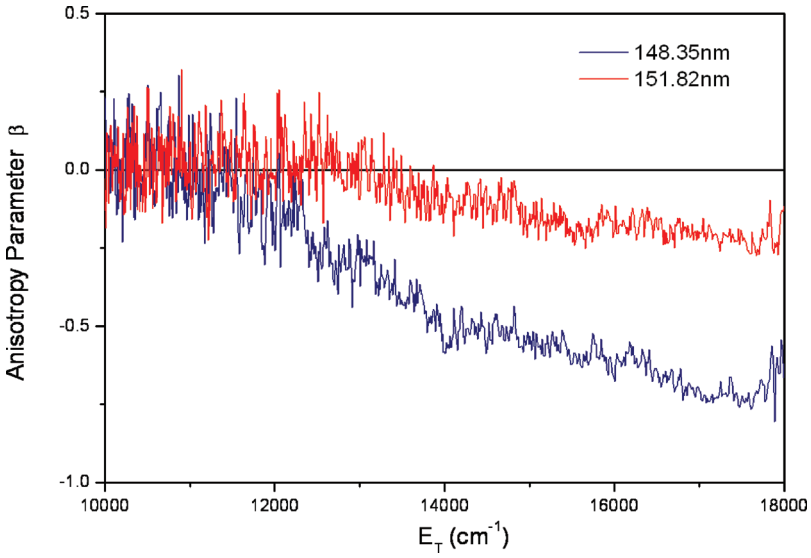

FIG. 4. The corresponding anisotropy distribution and anisotropy parameter value β from photolysis at 148.35 and 151.82 nm.

C_2H radicals. As the translational energy decreases, the anisotropy parameter also decreases until it reaches zero around E_T=11 000 cm^{-1}. This implies that the vibrationally excited $C_2H(\tilde{A}\ ^2\Pi)$ products are produced with much reduced angular anisotropy. For the 151.82 nm photolysis, the anisotropy parameter is significantly smaller, suggesting that the photodissociation process is a less direct process with a less vibrationally excited precursor. The translational energy dependence of the angular anisotropy is, however, quite similar for photolysis at both wavelengths.

C. Photodissociation dynamics

The electronically excited $\tilde{C}\ ^1\Pi_u$ state of acetylene is a Rydberg state that has a very fast predissociation. The equilibrium geometry of the acetylene $\tilde{C}\ ^1\Pi_u$ state is linear, so is the $C_2H(\tilde{A}\ ^2\Pi)$ product (Fig. 5).[37] From the spectroscopic studies, the $\tilde{C}\ ^1\Pi_u$ state is a strongly predissociative state.[22,30] The 151.82 nm peak (0_0^0 band) has a linewidth of 112 cm^{-1}, which corresponds to the predissociation lifetime of about 47 fs. The fast dissociation dynamics observed for photolysis via this band in the above experiment is clearly consistent with the fast predissociation lifetime. For the 148.35 nm peak, the spectral width is 308 cm^{-1}. This peak consists of three components. The lifetime of these three components is from 22 to 39 fs.[22] This means that the predissociation for this peak is faster than that for 151.82 nm peak. This is consistent with the more negative product anisotropy parameter observed in the 148.35 nm photodissociation dynamics (Fig. 4). The photolysis experiment for this peak was carried out at 148.35 nm excitation, which is on the top of the 4_0^2 (*trans*-bending) vibronic band. From a dynamical point of view, *trans*-bending vibration excitation will make the dissociating H-atom moving away from the acetylene in a nonlinear geometry (Fig. 5), and the moving in the opposite direction of the partner will enhance bending excitation in the $C_2H(\tilde{A}\ ^2\Pi)$ product, which has been observed in the experiment. For the 148.35 nm photolysis, the C–C stretching vibration is also excited via the 2_0^1 vibronic transition, this stretching excitation could also produce more C–C stretching vibrationally excited $C_2H(\tilde{A}\ ^2\Pi)$ product. The extra peak assigned to the $\tilde{A}\ ^2\Pi(0,\ v_2,\ 2)$ progression in the translational energy distribution for the 148.35 nm photolysis is an indication of the effect of the C–C stretching vibration excitation. Another interesting observation in the dynamical measurement is that the anisotropy parameter get closed to zero as the translational energy decreases for both excitation wavelengths. The possible explanation is that the C_2H products with high internal energy are produced via a more bent transition state.

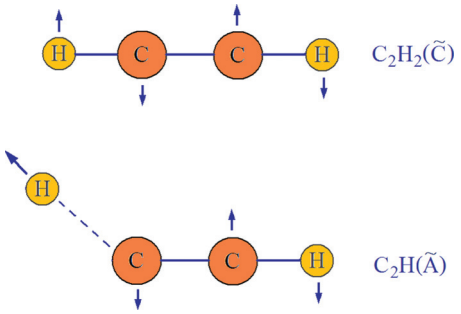

FIG. 5. The *trans*-bending vibration of the acetylene molecule and its likely effect on the dissociation process.

As for the dissociation route, it is not exactly clear which dissociative state is primarily responsible for the $\tilde{C}\ ^1\Pi_u$ predissociation. Previous spectroscopic study suggested that the $\tilde{C}'\ ^1A_g$ state might be responsible. This is unlikely the case since the "g" symmetry state cannot couple to u symmetry states via rovibronic couplings according to symmetry rules. Only nuclear spin effects can cause g/u mixing.[38] Furthermore, the $\tilde{C}'\ ^1A_g$ state is 7.7 eV above the ground state and only slight below the $\tilde{C}\ ^1\Pi_u$ state, it is not likely correlated with the $C_2H(\tilde{A}\ ^2\Pi)+H$ limit. In addition, the $\tilde{C}'\ ^1A_g$ state is bent, if dissociation occurs through this state, it should give much high rotational and bending vibration excitation, which is not the case in this work. Therefore, we believe that a valence dissociative state with u symmetry should be responsible for the $\tilde{C}\ ^1\Pi_u$ state predissociation. More clearly, the

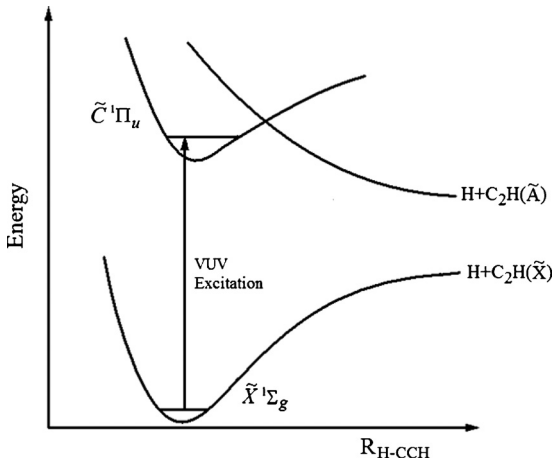

FIG. 6. Schematic photodissociation pathway for the acetylene molecule via the $\tilde{C}\,^1\Pi_u \leftarrow \tilde{X}\,^1\Sigma_g$ electronic excitation (Ref. 18).

dissociative state responsible for the $\tilde{C}\,^1\Pi_u$ state predissociation must be the excited state arising from $\pi \rightarrow 3s/\sigma^*$ excitation, which correlates diabatically with $H+C_2H(A)$ products, as discussed in the recent review of Ashfold *et al.*[29] From the experimental results, it is possible that the energy of 148.35 nm is more close to the nonadiabatic region, and the dissociation process is more fast and direct than that at 151.82 nm. It is, however, still not clear the detailed potential energy surface of the dissociative state how to effect the $\tilde{C}\,^1\Pi_u$ predissociation. Further theoretical studies are certainly needed in order to clarify this issue.

IV. CONCLUSIONS

Photodissociation dynamics of acetylene have been studied by means of HRTOF technique at laser radiation of 148.35 and 151.82 nm. The total translational energy distributions and angular distributions have been determined by measuring the H atom TOF spectra. The experimental results indicate that the $H+C_2H(\tilde{A})$ product channel is dominant process, while the $C_2H(\tilde{X}\,^2\Sigma^+)+H$ channel is a minor channel at most. The $C_2H(\tilde{A})$ product is excited in the C–C–H bending and C–C stretch vibration. Effect of precursor vibrational excitation on the product translational energy distribution has also been observed. The angular anisotropy for photodissociation (Fig. 6) at both wavelengths is found to be translational energy dependent; while the angular anisotropy distributions at both wavelengths are considerable different. This difference was also attributed to the effect of the C_2H_2 vibrational excitation on the dynamical process. The detailed pathway for the dissociation process is, however, not clarified, further theoretical studies are needed.

ACKNOWLEDGMENTS

This work was supported by the National Natural Science Foundation of China, the Ministry of Science and Technology of China, and the Chinese Academy of Sciences.

[1] Y. L. Yung, M. Allen, and J. P. Pinto, Astrophys. J., Suppl. Ser. **55**, 465 (1984).
[2] H. Okabe, Can. J. Chem. **61**, 850 (1983).
[3] R. D. Kern and K. Xie, Prog. Energy Combust. Sci. **17**, 191 (1991).
[4] S. Satyapal and R. Bersohn, J. Phys. Chem. **95**, 8004 (1991).
[5] K. K. Innes, J. Chem. Phys. **22**, 863 (1954).
[6] J. C. Van Craen, M. Herman, and R. Colin, J. Mol. Spectrosc. **119**, 137 (1986).
[7] J. D. Tobiason, A. L. Utz, E. L. Sibert III, and F. F. Crim, J. Chem. Phys. **99**, 5762 (1993).
[8] A. M. Wodtke and Y. T. Lee, J. Phys. Chem. **89**, 4744 (1985).
[9] B. A. Balko, J. Zhang, and Y. T. Lee, J. Chem. Phys. **94**, 7958 (1991).
[10] J. Zhang, C. W. Riehn, M. Dulligan, and C. Wittig, J. Chem. Phys. **103**, 6815 (1995).
[11] J. Segall, Y. Wen, R. Lavi, R. Singer, and C. Wittig, J. Phys. Chem. **95**, 8078 (1991).
[12] M. Fujii, A. Haijima, and M. Ito, Chem. Phys. Lett. **150**, 380 (1988).
[13] A. Haijima, M. Fujii, and M. Ito, J. Chem. Phys. **92**, 959 (1990).
[14] P. D. Foo and K. K. Innes, Chem. Phys. Lett. **22**, 439 (1973).
[15] J. Wang, Y. Hsu, and K. Liu, J. Phys. Chem. A **101**, 6593 (1997).
[16] P. Loeffler, E. Wrede, L. Schnieder, J. B. Halpern, W. M. Jackson, and K. H. Welge, J. Phys. Chem. A **109**, 5231 (1998).
[17] M. Suto and L. C. Lee, J. Chem. Phys. **80**, 4824 (1984).
[18] F. Laruelle, S. Boye-Peronne, D. Gauracq, and J. Lievin, J. Phys. Chem. A **113**, 13210 (2009).
[19] P. Forney, M. E. Jacox, and W. E. Thompson, J. Mol. Spectrosc. **170**, 178 (1995).
[20] P. G. Wilkinson, J. Mol. Spectrosc. **2**, 387 (1958).
[21] J. K. Lundberg, Y. Chen, J. P. Pique, and R. W. Field, J. Mol. Spectrosc. **156**, 104 (1992).
[22] Y. Hu, C. Zhen, J. Dai, X. Zhou, and S. Liu, Chin. J. Chem. Phys. **21**, 415 (2008).
[23] D. Demoulin and M. Jungen, Theor. Chim. Acta **34**, 1 (1974).
[24] J. O. Jensen, G. F. Adams, and C. F. Chabalowski, Chem. Phys. Lett. **172**, 379 (1990).
[25] J. Lievin, J. Mol. Spectrosc. **156**, 123 (1992).
[26] T. Nakayama and K. Watanabe, J. Chem. Phys. **40**, 558 (1964).
[27] A. Gedanken and O. Schnepp, Chem. Phys. Lett. **37**, 373 (1976).
[28] G. Cooper, G. R. Burton, and C. E. Brion, J. Electron Spectrosc. Relat. Phenom. **73**, 139 (1995).
[29] M. N. R. Ashfold, G. A. King, D. Murdock, M. G. D. Nix, T. A. Oliver, and A. G. Sage, Phys. Chem. Chem. Phys. **12**, 1218 (2010).
[30] A. Campos, S. Boye, P. Brechignac, S. Douin, C. Fellows, N. Shafizadeh, and D. Gauyacq, Chem. Phys. Lett. **314**, 91 (1999).
[31] H. J. Krautwald, L. Schnieder, K. H. Welge, and M. N. R. Ashfold, Faraday Discuss. Chem. Soc. **82**, 99 (1986).
[32] L. Schnieder, W. Meier, K. H. Welge, M. N. R. Ashfold, and C. M. Western, J. Chem. Phys. **92**, 7027 (1990).
[33] K. Yuan, L. Cheng, Y. Cheng, Q. Guo, D. Dai, and X. Yang, Rev. Sci. Instrum. **79**, 124101 (2008).
[34] K. Yuan, L. Cheng, Y. Cheng, Q. Guo, D. Dai, and X. Yang, J. Chem. Phys. **131**, 074301 (2009).
[35] D. H. Mordaunt and M. N. R. Ashfold, J. Chem. Phys. **101**, 2630 (1994).
[36] P. Löffler, D. Lacombe, A. Ross, E. Wrede, L. Schnieder, and K. H. Welge, Chem. Phys. Lett. **252**, 304 (1996).
[37] Q. Cui and K. Morokuma, J. Chem. Phys. **108**, 626 (1998).
[38] P. R. Bunker and P. Jensen, *Molecular Symmetry and Spectroscopy*, 2nd ed. (NRC Research, Ottawa, Canada, 1998).